

# Durable diamond-like carbon templates for UV nanoimprint lithography

L Tao<sup>1</sup>, S Ramachandran<sup>1</sup>, C T Nelson<sup>1</sup>, M Lin<sup>2</sup>, L J Overzet<sup>1</sup>,  
M Goeckner<sup>1</sup>, G Lee<sup>1</sup>, C G Willson<sup>2</sup>, W Wu<sup>3</sup> and W Hu<sup>1,4</sup>

<sup>1</sup> Department of Electrical Engineering, University of Texas at Dallas, Richardson, TX 75083, USA

<sup>2</sup> Department of Chemical Engineering, University of Texas at Austin, Austin, TX 78712, USA

<sup>3</sup> Quantum Science Research, HP Labs, Hewlett-Packard Company, Palo Alto, CA 94304, USA

E-mail: [walter.hu@utdallas.edu](mailto:walter.hu@utdallas.edu)

Received 26 October 2007, in final form 7 January 2008

Published 13 February 2008

Online at [stacks.iop.org/Nano/19/105302](http://stacks.iop.org/Nano/19/105302)

## Abstract

The interaction between resist and template during the separation process after nanoimprint lithography (NIL) can cause the formation of defects and damage to the templates and resist patterns. To alleviate these problems, fluorinated self-assembled monolayers (F-SAMs, i.e. tridecafluoro-1,1,2,2-tetrahydrooctyl trichlorosilane or FDTS) have been employed as template release coatings. However, we find that the FDTS coating undergoes irreversible degradation after only 10 cycles of UV nanoimprint processes with SU-8 resist. The degradation includes a 28% reduction in surface F atoms and significant increases in the surface roughness. In this paper, diamond-like carbon (DLC) films were investigated as an alternative material not only for coating but also for direct fabrication of nanoimprint templates. DLC films deposited on quartz templates in a plasma enhanced chemical vapor deposition system are shown to have better chemical and physical stability than FDTS. After the same 10 cycles of UV nanoimprints, the surface composition as well as the roughness of DLC films were found to be unchanged. The adhesion energy between the DLC surface and SU-8 is found to be smaller than that of FDTS despite the slightly higher total surface energy of DLC. DLC templates with 40 nm features were fabricated using e-beam lithography followed by Cr lift-off and reactive ion etching. UV nanoimprinting using the directly patterned DLC templates in SU-8 resist demonstrates good pattern transfer fidelity and easy template–resist separation. These results indicate that DLC is a promising material for fabricating durable templates for UV nanoimprint lithography.

(Some figures in this article are in colour only in the electronic version)

## 1. Introduction

Nanoimprint lithography (NIL), especially the ultraviolet (UV) version, has been considered by the semiconductor industry as one of the candidates for next generation manufacturing technology because of its high patterning resolution and low cost compared to state-of-the-art photolithography [1]. In UV-NIL, UV exposure is used to cure imprinted resist patterns in a template, allowing fast and room-temperature

processing without pattern distortion. In order to achieve high throughput, the scheme of step and flash imprint lithography (S-FIL), a scanner-like UV-NIL, is most promising [2]. Sequential step and imprint on large wafers will require precise alignment, durable and anti-sticky template surfaces, low defect density, and excellent pattern reproducibility. Due to the ‘contact printing’ nature of NIL, most of these issues are strongly related to the template–resist adhesion [3–5]. Currently, fluorinated self-assembled monolayers (F-SAMS), such as tridecafluoro-1,1,2,2-tetrahydrooctyl trichlorosilane (FDTS; Gelest) [3], are widely used to coat the templates,

<sup>4</sup> Author to whom any correspondence should be addressed.

resulting in super-hydrophobic surfaces to prevent resist sticking. However, F-SAMS gradually lose F atoms to the air and were recently found to chemically react irreversibly with UV-curable resists [6, 7]. This causes defects and even damage to the template, resulting in poor pattern reproducibility. The development of NIL templates with both chemical and physical stability is a necessity if UV-NIL is to meet the requirements for mass production of semiconductor and nanotech products.

In this study, the stability of F-SAMS coatings is further evaluated. Significant degradation of the F-SAMS coatings is observed after only 10 imprint cycles. Previously, we have developed diamond-like carbon (DLC) as an alternative template material with improved scratch and wear resistance for thermal NIL [8]. Here, we study the durability of the DLC template for UV nanoimprinting in comparison to the F-SAMS coating. The interfacial interaction of these coating layers with UV-curable SU-8 photo resist (Microchem) is investigated using surface characterization techniques. The experimental results of surface elemental composition, surface roughness, and surface energy indicate that the DLC coating offers much better chemical and physical durability than F-SAMS for UV-NIL. Nanostructures are then fabricated into the DLC films using e-beam lithography (EBL), metal lift-off, and reactive ion etching. Patterned DLC templates are then used in the UV imprint process to produce SU-8 nanoscale structures, which show high pattern transfer fidelity and easy release of the template from the resist. DLC is an ideal template material for nanoimprint templates because of its chemical inertness, low surface energy, UV transparency, and high hardness.

## 2. Experiments

### 2.1. DLC deposition and sample preparation

Si and quartz pieces were cleaned using acetone and then isopropyl alcohol in an ultrasonic agitation bath for 10 min. After blow-drying in N<sub>2</sub>, the samples were baked at 100 °C on a hot-plate for 2 min, and 20–100 nm thick DLC films were grown on the quartz samples using plasma enhanced chemical vapor deposition (PECVD). A mixture of methane (CH<sub>4</sub>) and argon in the ratio of 3:1 was used as the precursor. An inductively coupled plasma (ICP) system was used to deposit the DLC films in this work. This ICP system is more versatile than the capacitive coupled plasma (CCP) system used in our previous work [8]. It allowed us to sustain either a capacitive plasma (similar to our previous work) or an inductive plasma with or without capacitive power applied to the chuck. This latter allows the ion bombardment energy at the substrate surface to be controlled independently from the plasma creation and ion flux. Such independent control of ion density and flux to the surface (by ICP coil power) and ion bombardment energy (by 'wafer-chuck' or 'bias' power) enables a wider process test window through increased process control. Even so, one constraint in using the inductive plasma was ensuring low substrate surface temperatures and so we had to employ an intermittent plasma with an ON time of 15 s and OFF time of 30 s to obtain good films. We found that the DLC deposition rate is between 18 and 45 nm min<sup>-1</sup> for varying

bias powers of 10 W (–100 V self-bias) to 150 W (–590 V self-bias) and ICP coil powers (0–200 W). The DLC structure properties were characterized using Raman spectroscopy (not shown), indicating a sp<sup>3</sup>/sp<sup>2</sup> ratio of around 3:1 to 4:1 with hydrogen content of about 20–30%. We have prepared a set of 34 samples, 13 of which were deposited under CCP conditions (ICP coil power = 0) and 21 under ICP conditions (ICP coil power = 200 W). From the set of these films, we chose two with the best combination of UV transparency, surface energy, and hardness for imprint testing. These films were deposited under the following conditions: (a) ICP power = 0 W and bias power = 150 W (self-bias of –590 V) and (b) ICP power = 200 W and bias power = 10 W (self-bias of –100 V). A systematic study of the effects of the deposition conditions on film properties will be performed in a future work. In order to evaluate the imprint performance of DLC films in comparison to F-SAMS, quartz templates with FDTS coating were also prepared by immersing the quartz templates in FDTS solution in *n*-heptane for 5 min, followed by soaking in acetone for 2 min, N<sub>2</sub> blow dry, and baking on the hot-plate at 100 °C for 5 min. Both films were stored in the N<sub>2</sub> box before and after experiments.

### 2.2. UV-NIL

300 nm thick SU-8 ( $T_g \sim 55^\circ\text{C}$ ) was spin-coated onto Si samples followed by baking on a hot-plate at 65 °C for 1 min, 95 °C for 2 min, and 65 °C for 1 min. UV-NIL processes were carried out on an Obducat 2.5 nanoimprinter at a pressure of 1.5–6 MPa and a temperature of 25–75 °C. A UV light source with a broad spectrum output (250–450 nm) and a power of 40–100 mJ cm<sup>-2</sup> at the sample was used to expose the SU-8 resist for 3 s. FDTS and DLC coated quartz samples were used as blank templates and 10 UV-NILs were carried out continuously without cleaning the templates at the same imprinting conditions. UV-NIL using patterned DLC templates were also performed on SU-8 coated samples under similar imprint conditions.

### 2.3. Surface characterization

Surface properties of the FDTS and DLC films before and after the 10 UV-NIL cycles were characterized using x-ray photoelectron spectroscopy (XPS). XPS data were collected using a PHI 5701 LSci instrument with a monochrome Al K $\alpha$  (1486.6 eV) source and an analysis area of about 2.0 mm  $\times$  0.8 mm. Because the quartz samples are not conductive, charge correction was carried on correspondingly for FDTS and DLC samples. Contact angles of water and ethylene glycol on the FDTS and DLC films were measured using a Ramè Hart goniometer. Their surface energies were then calculated using a two-liquid method [9]. The optical transmission of the samples was measured using an n&k analyzer 1200RT/Iris 200. The surface roughness of the samples was investigated using a Veeco atomic force microscope (AFM). On each sample, root mean square (RMS) roughness was obtained by averaging over 5  $\mu\text{m}^2$  areas at three different locations.

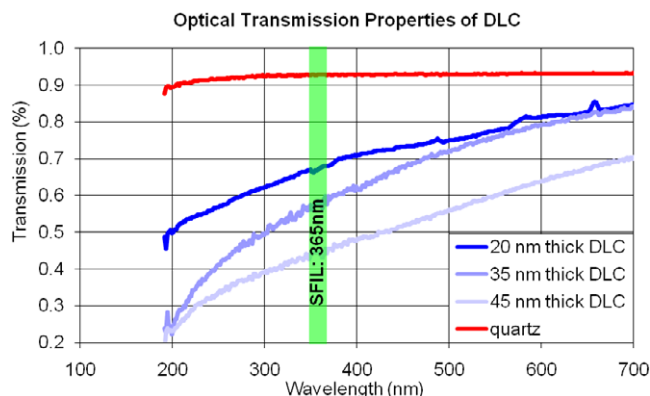


**Figure 1.** The transmission spectra of 20–45 nm DLC films on 1/4 in thick quartz S-FIL templates. The 20 nm film was deposited at zero coil power, 150 W bias power, and a gas pressure of 50 mTorr. The 45 nm film was deposited at zero coil power, 150 W bias power, and a gas pressure of 40 mTorr. The 35 nm film was deposited at 200 W ICP coil power, 10 W bias power, and a gas pressure of 40 mTorr. The optical absorbance of the films at the 365 nm wavelength were  $11.0$ ,  $9.9$ , and  $8.7 (\times 10^4 \text{ cm}^{-1})$  for the 20, 45, and 35 nm films, respectively.

#### 2.4. Fabrication of the DLC template

The DLC template was fabricated using EBL, metal lift-off, and then a reactive ion etching process. Nanoscale gratings of 40 nm width and spacing were formed in a polymethylmethacrylate (PMMA) resist on the DLC coated quartz samples using EBL. Typical EBL processes used a beam energy of 30 keV, an aperture of 15  $\mu\text{m}$ , a beam current of 200 pA, a working distance of 5 mm, and cold development in methyl isobutyl ketone:isopropyl alcohol (1:3) with 1.5% methyl ethyl ketone [10]. After the development of PMMA patterns, 10 nm thick Cr was evaporated on the sample and a lift-off process was performed in acetone in an ultrasonic bath for 5 min to transfer the PMMA patterns to the Cr layer. Using the Cr gratings as a mask, reactive ion etching using pure  $\text{CF}_4$  was performed in a home-made ICP system with an ICP power of 400 W, DC bias of 100 V,  $\text{CF}_4$  35 sccm, and 15 mTorr, as discussed in previous work [8]. After the Cr residue was stripped away, patterned DLC nanostructures were evaluated using AFM and then used as a template in the UV-NIL processes.

### 3. Results and discussion

#### 3.1. UV transmittance

In the S-FIL or UV-NIL process, UV light with wavelength around 365 nm is transmitted through the template to cure the photoresist underneath. The template transmittance at this wavelength is important for the throughput and power efficiency of the process. Figure 1 shows the transmission spectra of the S-FIL templates coated with 20–45 nm thick DLC deposited using different PECVD conditions in comparison to a bare quartz template. The 20 nm DLC coated quartz template provides close to 70% transmittance around the 365 nm wavelength of interest. The 20 and 45 nm thick

DLC films in figure 1 were deposited using only CCP (ICP power = 0 W, bias power = 150 W, and self-bias of  $-590$  V) for different lengths of time. The 35 nm film was deposited using ICP (ICP power = 200 W, bias power = 10 W, and self-bias of  $-100$  V). As shown in figure 1, the films deposited using CCP and ICP show different absorbance characteristics in the UV range. The ICP deposited DLC film has a somewhat higher C–H concentration and therefore higher absorbance at shorter wavelengths (e.g. around 200 nm) but lower absorbance at longer wavelengths (e.g. 365 nm), compared to the 20 nm and 45 nm samples deposited with zero ICP power. For the 365 nm UV light of interest, the optical absorption ( $\alpha$ ) of the 35 nm DLC is the lowest ( $8.7 \times 10^4 \text{ cm}^{-1}$ ), offering the best transparency, in comparison to the 20 nm ( $\alpha \sim 11 \times 10^4 \text{ cm}^{-1}$ ) and 45 nm samples ( $\alpha \sim 9.9 \times 10^4 \text{ cm}^{-1}$ ). It was also observed that a lower plasma pressure results in better transparency for the same deposition power. In addition, increasing the coil power further at a constant bias power appeared to increase the polymerization of the precursor and lead to softer films with a higher hydrogen content. Further, increasing the bias power (holding the ICP coil power constant) appeared to increase the  $\text{sp}^2$  fraction in the film leading to more graphitic films that have reduced hardness and transmittance. The window for films with good properties was found to be  $200 \pm 100$  W for the ICP coil power and  $-100 \pm 50$  V for the DC self-bias at the particular flow and pressure (40 mTorr) conditions that we employed.

We understand that the optical transmittance of DLC films can be further enhanced by maintaining a narrow ion energy distribution around 100–150 eV, resulting in a high content of  $\text{sp}^3$  C–C bonding due to the surface kinetics of the carbon deposition [11]. A lower chamber pressure (e.g. 10 mTorr) and a precursor with lower hydrogen content (e.g.  $\text{C}_2\text{H}_2$ ) can be used, which will be explored in future work. The high transmittance of thick DLC films is promising since nanostructures can be directly fabricated in the DLC films instead of coating DLC on the patterned quartz templates, for which uniform step coverage is quite difficult. The patterning of DLC films is discussed in section 3.4. The presented PECVD process was chosen for the desired DLC properties and has relatively poor step coverage. It may be that the conditions can be optimized to improve step coverage if needed.

#### 3.2. Characterization of surface chemistry

XPS elemental concentrations for both FDTS and DLC surfaces before and after the 10 cycles of UV-NILs are shown in table 1. Samples denoted as ‘FDTS0’ and ‘FDTS10’ refer to FDTS coated quartz templates with zero and 10 UV-NIL imprint cycles, respectively. Similarly, 100 nm DLC coated quartz templates are denoted as ‘DLC0’ and ‘DLC10’. In addition, figure 2 shows the XPS spectra of the FDTS0 and FDTS10 samples. From table 1, the most noticeable change in the atomic composition is a reduction of the F atom by  $\sim 28\%$  after the UV-NIL. There are pronounced changes on the peak and areas of C–C,  $\text{CH}_2\text{–CF}_2$ ,  $\text{CF}_3$ , and  $\text{CF}_2$  in the spectra of the FDTS10 sample (figure 2(b)) compared to FDTS0

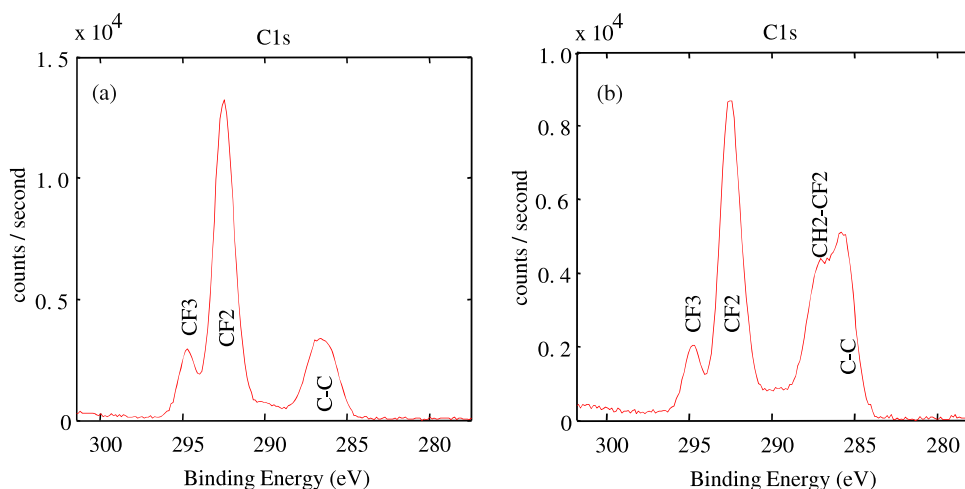


**Figure 2.** XPS spectra of the FDTS coated quartz surface (a) before and (b) after 10 cycles of UV nanoimprints.

**Table 1.** Atomic concentrations (at.%) (Normalized to 100% of the elements detected. XPS does not detect H or He.) of the template surfaces before and after 10 cycles of UV-NIL.

Sample	Element concentration (%) <sup>a</sup>				
	C	N	O	F	Si
FDTS0	17.0	0.1	28.5	37.9	16.5
FDTS10	17.5	0.3	35.5	27.4	19.3
DLC0	85.7	1.3	12.9	0.0	0.0
DLC10	83.7	1.0	14.6	0.1	0.6

<sup>a</sup> The precision of the quantitative data is 3–5% for the elements present at concentrations > 10 at.%.

(figure 2(a)). To quantify these changes, the decomposition of the carbon 1s spectral curves for the FDTS samples is shown in table 2 with the integrated area (%) for each component. The area% at 286 eV (C–C) and 287 eV (CH<sub>2</sub>–CF<sub>2</sub>) increased significantly, while the area% of 293 eV (CF<sub>2</sub>) and 295 eV (CF<sub>3</sub>) decreased after the imprint. In other words, the imprint caused the significant increase of the area ratio C–C/CH<sub>2</sub>–CF<sub>2</sub> to CF<sub>2</sub>/CF<sub>3</sub>, indicating the loss of F atoms through the interfacial interaction between FDTS and SU-8 during the UV exposure. It is known that the SiCl<sub>3</sub> group of FDTS can attach to the quartz surface even without the presence of water because the electron (e<sup>-</sup>)-withdrawing effect of the fluoro group makes Si a better electrophile for nucleophilic attack by O from the hydroxyl group [12]. For the same reason, the CF<sub>3</sub> group is likely to react with e<sup>-</sup>-providing group or radicals from the epoxy groups from the SU-8 under UV exposure, resulting in the formation of volatile F-containing species, followed by their escaping from the FDTS surface. This explanation agrees with previously reported observation about F-atom abstraction from fluorocarbons by radicals [12–15] and volatile F-containing species escaping from the F-SAMs after imprinting with UV-curable resists [6]. The degradation of the FDTS film caused the exposure of the underneath quartz surface to the XPS measurements, resulting in the increased O and Si concentration. These results indicate that significant

**Table 2.** The carbon 1s spectral curve decomposition of the FDTS samples before and after 10 cycles of UV-NIL.

FDTS0		FDTS10	
Peak position (eV)	Area (%)	Peak position (eV)	Area (%)
286.04	11.67	285.67	25.03
287.08	11.24	287.25	20.01
289.43	2.10	289.14	3.44
290.95	2.55	290.95	3.19
292.48	62.18	292.50	41.65
294.72	10.26	294.80	6.68

damage of the FDTS coating occurred after 10 cycles of UV-NIL even at room temperature and low pressure (1.5 MPa). The chemical attack problem for FDTS coating under the UV exposure has also been reported for methacrylate, vinyl ether, and acrylate resists [6, 7].

Compared to FDTS, the changes in the elemental composition of DLC surfaces (table 1) and the C 1s spectra (figure 3) before and after 10 cycles of UV imprinting are quite small. A slight increase in the O and Si content was observed. This may be due to the replacement of the hydrogen in the DLC films by O and possible airborne particles on the surface. Other changes in the elemental composition are within the measurement error range. These results demonstrate that DLC has a higher chemical and physical stability than FDTS for nanoimprint template coating.

### 3.3. Surface roughness, energy, and adhesion strength

AFM measurements in figure 4 show that the roughness of uniform FDTS and DLC coated quartz templates is 0.3 nm and 0.2 nm, respectively, before the UV imprinting; these values are close to the roughness of the original quartz surface (~0.2 nm). After 10 UV-NIL cycles, the surface roughness of the FDTS coated quartz increased to about 1.0 nm, which is close to the thickness of the FDTS film. This observation further proves the microscopic damage of FDTS coating by the UV imprint process. In comparison, the UV-NIL generated a slight increase (from 0.2 to 0.4 nm) in the DLC roughness, as

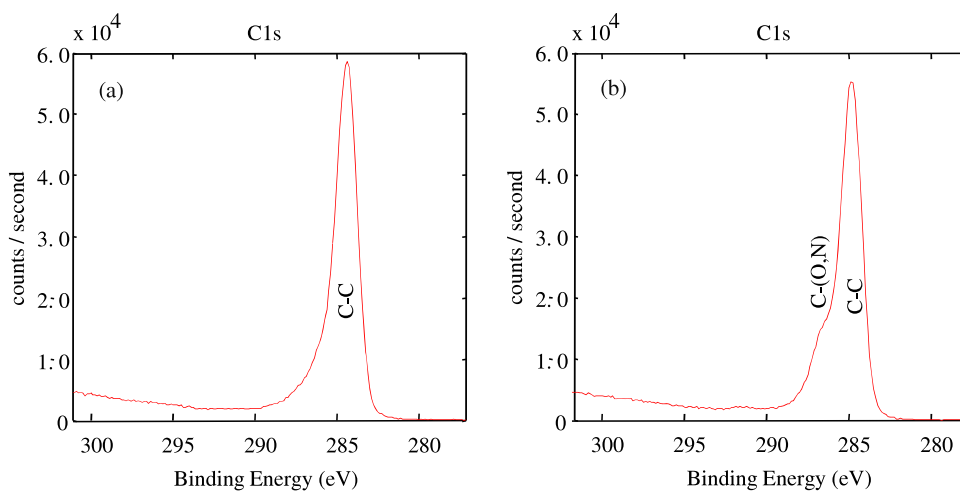


Figure 3. XPS spectra of the DLC coated quartz surface (a) before and (b) after 10 cycles of UV nanoimprinting.

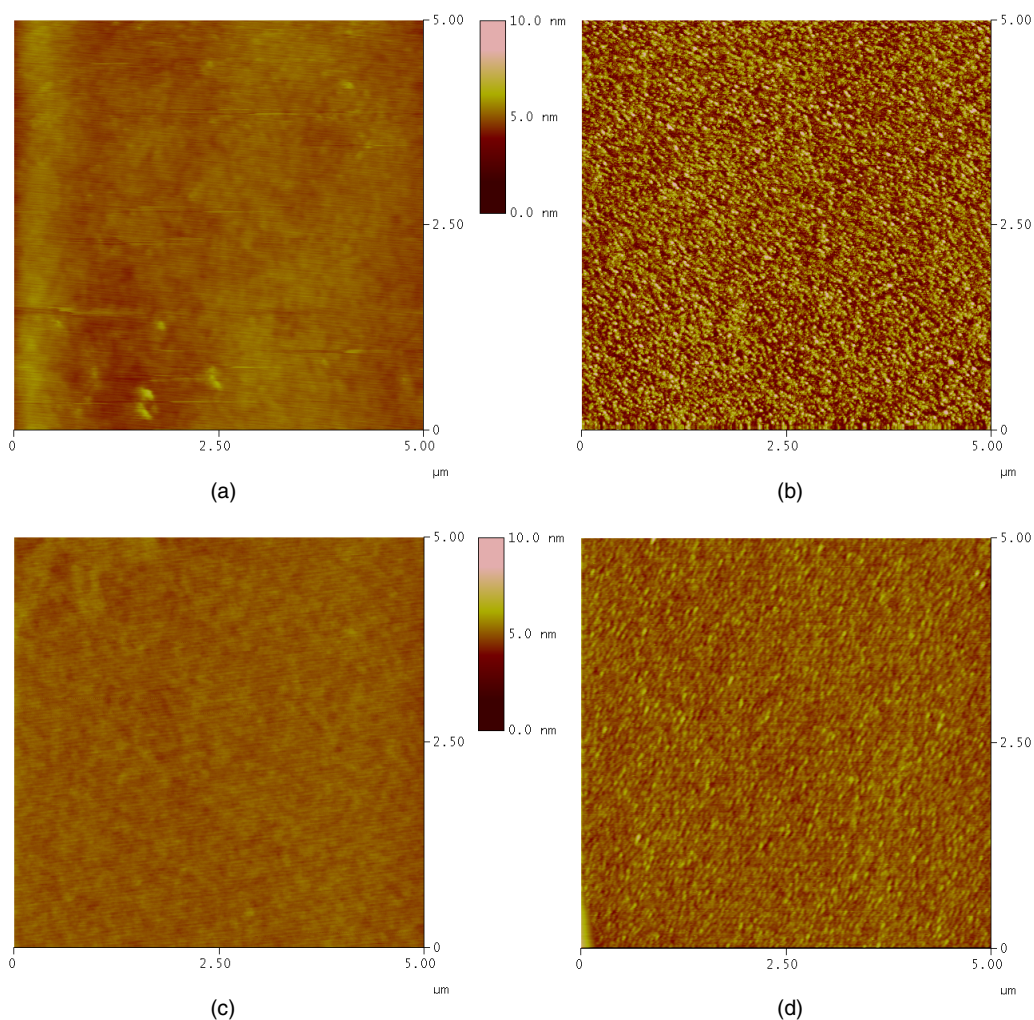
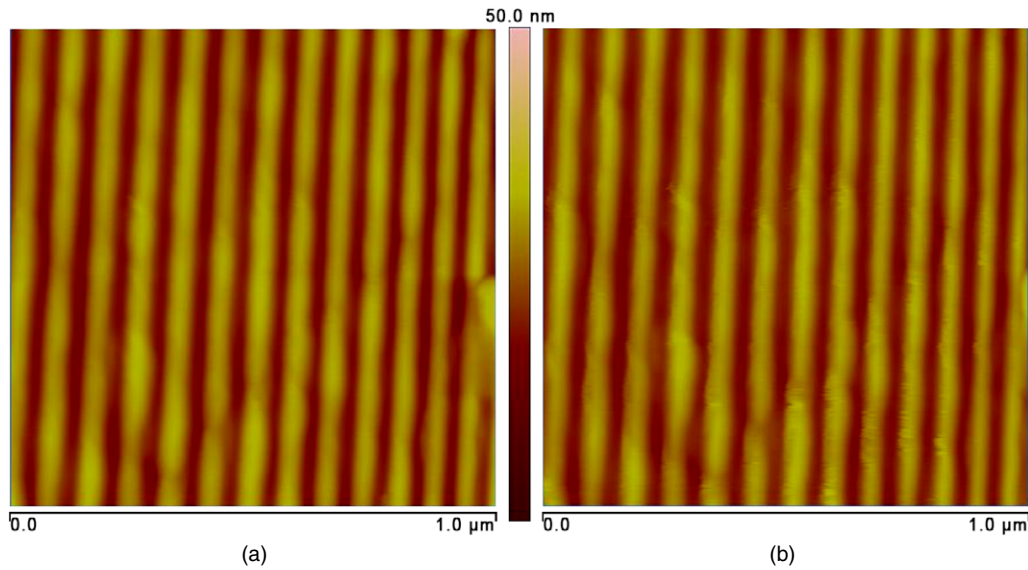


Figure 4. AFM images of the FDTD coated quartz surface (a) before and (b) after 10 cycles of UV nanoimprinting; (c) the DLC coated quartz surface before and (d) after the 10 cycles of UV nanoimprinting.

shown in figures 4(c) and (d), indicating a better stability for the DLC coating than the FDTD.

Table 3 shows the data of contact angle measurements and the calculated surface energies of the quartz, FDTD, and DLC

surfaces before and after the 10 cycles of UV-NIL. The DLC films and FDTD coating have comparable low surface energies. In addition, the surface energies of both films are stable before and after UV-NIL. Apparently, the surface energy data cannot



**Figure 5.** AFM images of (a) the nanostructured DLC template with 40 nm wide 100 nm deep gratings and (b) the imprinted SU-8 structures.

**Table 3.** Contact angles and calculated surface energies for the FDTS and DLC films before and after the UV-NIL and for the UV-cured SU-8 resist.

Samples	Contact angle (deg)		Surface energy <sup>a</sup> ( $\gamma = \gamma^d + \gamma^p$ ) ( $\text{mJ m}^{-2}$ )		
	H <sub>2</sub> O	Ethylene glycol	$\gamma^p$	$\gamma^d$	$\gamma$
	FDTS0	91.6 ± 0.7	63.0 ± 0.9	2.3	27.5
FDTS10	92.4 ± 0.9	65.5 ± 1.0	2.6	24.9	27.5
DLC0	66.4 ± 0.9	45.8 ± 0.9	21.7	14.4	36.1
DLC10	63.4 ± 0.7	44.5 ± 0.5	25.6	12.6	38.2
Quartz	32.5 ± 0.7	25.5 ± 1.2	67.0	3.5	70.5
Cured SU-8	80.0 ± 0.7	43.0 ± 0.5	4.0	37.2	41.2

<sup>a</sup> Surface energy  $\gamma$  is the sum of  $\gamma^d$  (dispersion or non-polar component) and  $\gamma^p$  (polar component).

reveal the microscopic damage to the FDTS films, as shown in previous sections. However, it does provide information about the resist adhesion to the templates and the energy needed to release the template from the resist. The adhesion energy ( $W_{AB}$ ) between the template and resist can be estimated using the Owens and Wendt geometric mean approach [9]:

$$W_{AB} \cong \sqrt{\gamma_A^p \cdot \gamma_B^p} + \sqrt{\gamma_A^d \cdot \gamma_B^d} \quad (1)$$

where  $\gamma^p$  and  $\gamma^d$  represent the polar and dispersive (or non-polar) components, respectively, of the surface energies of the two materials in contact. The adhesion energies of cured SU-8 to FDTS ( $W_{\text{FDTS/SU-8}}$ ) and to DLC ( $W_{\text{DLC/SU-8}}$ ) are calculated to be 33.7  $\text{mJ m}^{-2}$  and 31.7  $\text{mJ m}^{-2}$ , respectively, by plugging corresponding values from table 3 into equation (1). It shows that the adhesion energy of SU-8 to the DLC films is slightly lower than that of the FDTS although the DLC has a higher surface energy than FDTS. Therefore, the DLC templates are actually easier (or at least similar) to separate from the cured SU-8 than FDTS, as observed in the imprint experiments. The

adhesion of resist to the template is highly resist dependent. Most resists have a high non-polar component and therefore would have low adhesion to DLC films since the DLC has a small non-polar surface energy, resulting in better release performance than FDTS. Similar experimental observation is reported for UV-cured methacrylate, vinyl ether, and acrylate resists [7].

#### 3.4. UV-NIL using nanostructured DLC templates

The AFM image in figure 5(a) shows 40 nm wide and 100 nm deep gratings fabricated in 300 nm thick DLC films using EBL, followed by metal lift-off and ICP etching, as described previously. The DLC etch rate was about 100  $\text{nm min}^{-1}$  and the roughness of the film was nearly the same before and after the etching [8]. The results demonstrate that direct nanopatterning of DLC is feasible and advantageous compared to the deposition of DLC on patterned quartz, which has relatively non-uniform step coverage and poor film stability due to higher interfacial stress and wearing. UV nanoimprinting processes were carried out with the patterned DLC template. Figure 5(b) shows the imprinted SU-8 gratings, which are measured with similar dimensions to the template, indicating good pattern transfer fidelity of the imprint process. The template release from the cured SU-8 structures is easy and no obvious pattern distortion has been observed. The patterned DLC templates have been constantly used for more than 6 months and their surface energies and film roughness are quite stable.

As shown in figure 1, the UV transmittance varies with DLC thickness and therefore the patterned DLC templates will result in spatially non-uniform UV exposure to the resist underneath. Such issues can be alleviated by depositing films using inductive plasmas with very low pressure and narrower ion energy distribution, as discussed in section 3.1. Moreover, the effect of this non-uniform exposure on pattern formation in resist is not significant since the resist patterns are defined

by polymer filling to the template concaves not by the UV exposure as in photolithography. In nanoimprinting, the UV exposure is only used to cure resist patterns and the exposure time was chosen to ensure that the resist under the thick DLC patterns gets a sufficient dose. In addition, DLC films are known to be excellent candidates as protective coatings on things like magnetic hard drives, primarily because the hardness of films above a few nm does not show significant dependence on the thickness [11]. Hence the uniformity of the hardness with thickness may not be a problem for structures with spatial variation in thickness.

#### 4. Summary

Fluorinated SAM-coated quartz templates were found to be chemically reactive to the radicals generated from the SU-8 resist under UV exposure, resulting in film degradation and roughened surfaces after only 10 cycles of a UV nanoimprinting processes. This kind of irreversible chemical damage limits the future applications of F-SAMS as template release coatings for nanoimprint lithography. DLC films were investigated as a promising alternative template material. DLC films were deposited on the quartz templates using plasma enhanced chemical vapor deposition and characterized using XPS and AFM before and after UV nanoimprinting in comparison to the FDTS films. The elemental composition, surface roughness, and surface energy of the DLC films are quite stable. The adhesion energy of the DLC template to SU-8 is smaller than that of FDTS despite its slightly higher surface energy. DLC templates with 40–50 nm feature size were fabricated using EBL followed by Cr lift-off and ICP etching. UV nanoimprinting using patterned DLC templates in SU-8 shows excellent pattern transfer fidelity at the nanoscale. We believe the DLC material is a promising coating layer and

can also be directly patterned as nanoimprint templates with high chemical stability and high wear resistance.

#### Acknowledgments

The authors would like to thank Professor Robert M Wallace and student Bongki Lee at The University of Texas at Dallas for the discussion on XPS spectrum analysis.

#### References

- [1] 2003–2006 International Technology Roadmap for Semiconductors <http://www.public.net/itrs>
- [2] Colburn M *et al* 1999 *Proc. SPIE* **3676** 379
- [3] Bailey T, Choi B J, Colburn M, Meissl M, Shaya S, Ekerdt J G, Sreenivasan S V and Willson C G 2000 *J. Vac. Sci. Technol. B* **18** 3572
- [4] Otto M, Bender M, Richter F, Hadam B, Kleim T, Jede R, Spangenberg B and Kurz H 2004 *Microelectron. Eng.* **73/74** 152
- [5] Jung GY, Li Z, Wu W, Chen Y, Olynick D L, Wang S Y, Tong W M and Williams R S 2005 *Langmuir* **21** 1158
- [6] Houle F A, Guyer E, Miller D C, Dauskardt R, Rice E and Hamilton J 2006 *Proc. SPIE* **6153** 61531B
- [7] Houle F A, Rettner C T, Miller D C and Sooriyakumaran R 2007 *Appl. Phys. Lett.* **90** 213103
- [8] Ramachandran S, Tao L, Lee T H, Sant S, Overzet L J, Goeckner M J, Kim M J, Lee G S and Hu W 2006 *J. Vac. Sci. Technol. B* **24** 2993
- [9] Owens D K and Wendt R C 1969 *J. Appl. Polym. Sci.* **13** 1741
- [10] Hu W, Bernstein G H, Sarveswaran K and Lieberman M 2004 *J. Vac. Sci. Technol. B* **22** 1711
- [11] Robertson J 2002 *J. Mater. Sci. Eng. R* **37** 129
- [12] Tripp C P, Veregin R P N and Hair M L 1993 *Langmuir* **9** 3518
- [13] Tasker S, Chambers R D and Badyal J P S 1994 *J. Phys. Chem.* **98** 12442
- [14] Morgan A M, Evans B and Kells J 1995 *Langmuir* **11** 4393
- [15] Kochi J (ed) 1973 *Free Radicals* (New York: Wiley–Interscience)